Pergamon

Polyhedron Vol. 14, No. 23–24, pp. 3515–3518, 1995
Copyright © 1995 Elsevier Science Ltd
Printed in Great Britain. All rights reserved
0277–5387/95 $9.50+0.00

0277-5387(95)00203-0

OXYGEN STATES IN THE CASE OF INTERACTION OF O_2 WITH METAPHOSPHATE MELTS CONTAINING 3D-METAL IONS

SERGEY V. VOLKOV, VICTOR A. BANDUR* and NIKOLAY I. BURYAK

Institute of General and Inorganic Chemistry of the Ukrainian National Academy of Sciences, 32–34, Pr. Palladina, Kiev-142, 252680, Ukraine

(*Received* 20 *February* 1995; *accepted* 24 *April* 1995)

Abstract—Interaction between atmospheric oxygen, the air–methane mixture and methane, on the one hand, and $NaPO_3$ melt and binary $NaPO_3$–CoO, $NaPO_3$–Sc_2O_3 and $NaPO_3$–ZnO melts, on the other hand, has been studied by electron absorption (EA), electron spin resonance (ESR) and IR spectroscopy. The formation of different types of superoxide ions has been revealed: O_2^- in $NaPO_3$ ($g = 2.000$) and $O_2^{\delta\dot{-}}$ ($g = 1.921$ and 1.924) in the oxygenated $[(PO_3^-)_y M \cdot O_2^{\delta\dot{-}}]$ complex (where $M = Co^{2+}$, Zn^{2+}) with electron density delocalized between ions of the complexing metal and $O_2^{\dot{-}}$.

As we have previously shown,[1–3] sodium metaphosphate melts containing some *d*-metal ions are promising as catalysts of partial oxidation of the most unreactive alkane–methane compounds.

A mass spectrometry study of oxygen exchange processes between the air and melt, with and without catalytically active 3*d*-metal complexes, enabled us to establish that the exchange proceeds between the atoms of molecular oxygen dissolved in the melt and oxygen atoms of metaphosphate groups of the melt.[4] This means, of course, dissolution, as the first stage, and interaction between molecular oxygen and the melt of sodium metaphosphate. As previously shown,[5] an electron absorption spectrum of individual molten sodium metaphosphate has the edge of the intensive band of intramolecular (PO_3^-) transfer at 45,000 cm^{-1} with a shoulder at *ca* 40,000 cm^{-1}, which is due to the presence of residual oxygen dissolved in the melt. Identification of the spectra is also given in this work. At high concentration of dissolved oxygen a broadening of the absorption zone up to 30,000 cm^{-1} was observed in the EA spectra, which is caused by a variety of chain, cyclic and other polyphosphate forms giving the $(PO_3^-)_x O_2$-type groups in the melt.

In this work we have investigated the interaction of atmospheric oxygen, an air–methane mixture and methane with an individual $NaPO_3$ melt and binary $NaPO_3$–CoO, $NaPO_3$–Sc_2O_3 and $NaPO_3$–ZnO melts by EA, ESR and IR spectroscopy to ascertain the state of oxygen dissolved in such melts.

EXPERIMENTAL

The interaction between gases and melts was carried out at a temperature of 850°C. Electron absorption spectra were recorded using the Specord UV–vis spectrophotometer in a high-temperature quartz cell with a thickness of absorbing layer of 5 mm. ESR spectra of fast-quenched melts were taken with the use of the RE-1306 spectrometer, whereas IR spectra were recorded with the UR-20 instrument. Previous studies[6] proved the reasonableness of such a technique as fast quenching for interpretation of processes proceeding in a melt. All the reactants used were of chemical purity grade.

RESULTS AND DISCUSSION

Considering the interaction between the individual $NaPO_3$ melts and air, methane and their

---

* Author to whom correspondence should be addressed.

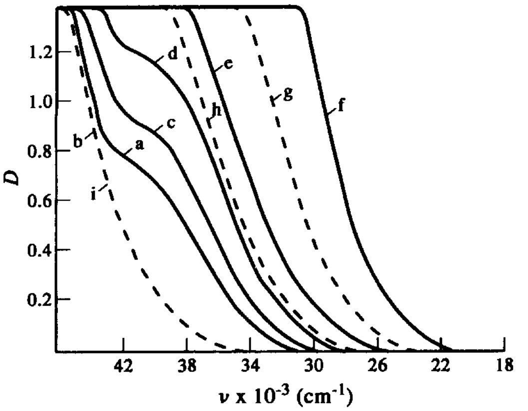

Fig. 1. Electron absorption spectra at 650°C: (a) $NaPO_3$ melt; (b) taken after the removal of residual oxygen by blowing helium (3600 s); (c)–(f) taken after passing the atmospheric oxygen through the melt for 5, 15, 1800 and 5400 s, respectively; (g)–(i) taken after the removal of oxygen by blowing helium for 300, 900 and 3600 s, respectively.

mixture, it should be expected in the individual quenched $NaPO_3$ melt that no ESR signal is observed either before or after bubbling methane through the melt (see Table 1). In passing the air or air–methane mixture through the quenched melt an ESR signal is observed as a single line with $g = 2.000$ and a width of 38 G (Table 1).

Simultaneously, an absorption band at 1140–1150 cm^{-1} has been revealed in the IR spectrum of these quenched $NaPO_3$–O_2 melts. Since the upper filled molecular orbitals (MOs) of PO_3^- ions are energetically located in the same region as the half-filled antibonding $1\pi_g^*$ MO of molecular oxygen, then conditions for the electron transition from MO $PO_3^-(\pi)$ to $1\pi_g^*$ MO O_2, shown by EAS data, can be realized. In the case of complete electron transfer, one of the possible results will be formation of a superoxide species or anion-radical $O_2^{\dot{-}}$. Actually, the frequency *ca* 1145 cm^{-1}, reported previously[7] and revealed in our work, is referred to as just the valence vibration of the O—O bond in $O_2^{\dot{-}}$, because the valence vibration of the O—O bond of molecular oxygen (1556 cm^{-1}) is not observed in the IR spectrum.

Although O_2 is also a paramagnetic molecule possessing two unpaired electrons (biradical) it has been shown by an ESR study of molecular oxygen in nitrogen and argon matrices that a narrow (up to 70 G in the 3 cm SWF range) asymmetrical ESR signal attributed to molecular oxygen ($g_\perp = 2.02 \pm 0.02$; $g_\parallel = 0.7$) at fields of *ca* 11 KG broadens with temperature, and at a temperature of *ca* 23 K its detection becomes impossible.[8]

As a result of the assumed formation of the superoxide ion $O_2^{\dot{-}}$ in the $NaPO_3$ melt, antibonding and lengthening of the oxygen–oxygen bond proceeds with a corresponding decrease in its dissociation energy:[9]

Species	R(O—O) (nm)	D (kJ mol^{-1})	ν(O—O) (cm^{-1})
O_2	120.7	493.59	1556
O_2^-	128.0	407.81	1145

The formation of superoxide ions in the $NaPO_3$ melt is also shown by the presence of an EAS band in the region 40,000 cm^{-1}, which is attributed to $O_2^{\dot{-}}$ both in our[7] and some other previous reports.[10]

Considering the $NaPO_3$ melt containing *d*-metal ions, passing air through the $NaPO_3$–CoO melt,

Table 1. ESR signals of quenched samples of melts.

Sample	Bubbling time (min)	g-factor, 20°C	Width of ESR line, (G)
$NaPO_3$	—	—	—
$NaPO_3$–CoO	—	—	—
$NaPO_3 + O_2$	30	2.000	38
($NaPO_3$–CoO) + O_2	30	2.000	38
$NaPO_3 + CH_4$	30	—	—
$NaPO_3 + CH_4 + O_2$	20 + 15	2.000	38
($NaPO_3$ + CoO) + CH_4	20	—	—
($NaPO_3$–CoO) + $CH_4 + O_2$	20 + 15	1.921	50
($NaPO_3$–CoO) + ($2CH_4 + O_2$)	30	1.921	50
$NaPO_3$–Sc_2O_3	—	—	—
($NaPO_3$–Sc_2O_3) + $CH_4 + O_2$	60 + 60	—	—
$NaPO_3$–ZnO	—	—	—
($NaPO_3$–ZnO) + $CH_4 + O_2$	30 + 30	1.924	42

whose ESR signal is not fixed, leads to the appearance of an ESR signal with $g = 2.000$, similar to that obtained for the $NaPO_3$–O_2 system (Table 1), and to such a strong absorption up to 30,000 cm^{-1} as in the case of individual $NaPO_3$ melt.[5] However, in contrast to reversible deoxygenation of the individual $NaPO_3$ melt first saturated with oxygen and then degassed by blowing helium, for the $NaPO_3$–CoO–O_2 system no complete deoxygenation of the melt has been reached, and the edge of its absorption band in prolonged bubbling helium or nitrogen through the melt did not return to the initial position [Fig. 2(d)]. It is most likely to be due to the $O_2^{\dot{-}}$ species formed as a result of electron transfer from MO $PO_3^-(\pi)$ to $1\pi_g^*$MO O_2, which is also evidenced by the same width of their ESR lines (38 G). Therefore, in both cases, the presence of unbound superoxide ions is fixed in the melt. In passing methane undergoing an oxidation reaction through the melt, the complete deoxygenation of the latter is observed, and the edge of the EAS band returns to its initial position [Fig. 2(e)].

Quite another picture is observed when the $NaPO_3$–CdO melt is first bubbled with methane and then with air. In the latter case, another ESR signal (with $g = 1.921$ and a width of 50 G) appears (Table 1). Our mass spectroscopy studies[4] can explain this fact. These studies have shown that at the first stage of dissolution of higher *d*-metal oxides in the melt of sodium metaphosphate there proceeds evolution of oxygen thermochemically formed as a result of the following redox reaction between *d*-metal ions and oxygen anions in the melt: $M^{n+} + O^{2-} \rightarrow M^{+(n-2)} + 1/2O_2$. Only on accumulating vacant coordination centres of partially reduced *d*-metal ions in the melt does the possibility of coordinating molecular oxygen with these centres arise. In subsequent bubbling through the melt, the atmospheric oxygen can occupy these vacant coordination centres and combine with the complexing metal to give an ESR signal with $g = 1.921$.

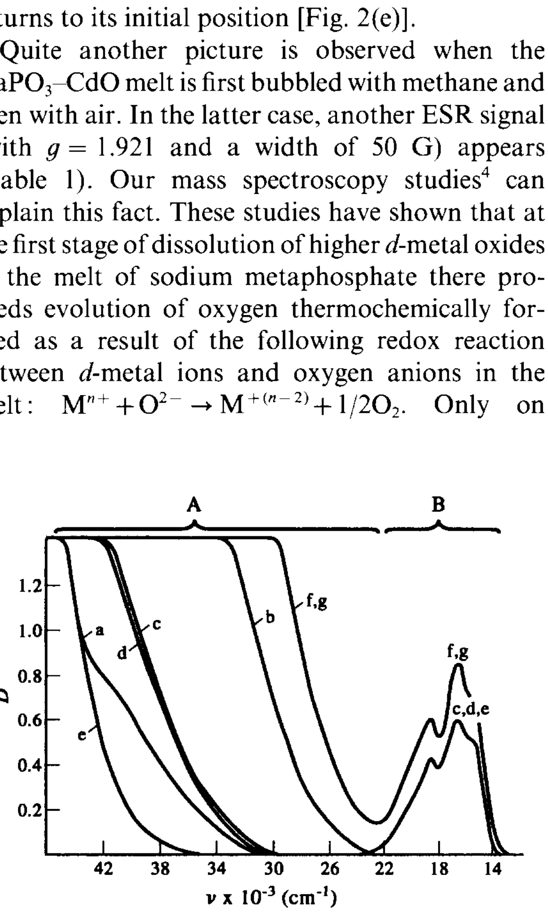

Fig. 2. Electron absorption spectra at 650°C: (a) $NaPO_3$ melt; (b) taken after passing the atmospheric oxygen through the melt for 3600 s; (c) $NaPO_3$+0.22 mol dm^{-3} CoO melt; (d) taken after blowing helium for 3600 s; (e) taken after passing methane for 3600 s; (f) taken after passing the atmospheric oxygen for 5400 s; (g) taken after passing the methane–air mixture for 3600 s.

As to the *d–d* spectra of polyphosphate complexes of cobalt [Fig. 2(B)] in molten $NaPO_3$ in the absence of dissolved oxygen and in its presence the difference in EAS is clearly seen. In the latter case, the *d–d* spectra are more intense and show, by the values of half-width of bands ($\delta_{1/2}$), broadening of the band. In this case, in $NaPO_3$ an equilibrium between tetrahedral and octahedral chromophores of cobalt(II) is observed. The equilibrium shifts with temperature towards the predominant tetrahedral chromophores[6] which possess much higher band intensities in the EAS. Also a great number of transitions are fixed in this region, e.g. for a tetrahedral polyphosphate polyhedron of cobalt: ${}^4A_2 \rightarrow {}^4T_1({}^4P)$ (17,000 cm^{-1}), ${}^4A_2 \rightarrow {}^2E,{}^2T_1,{}^2A_1,{}^2T_2({}^2G)$ (16,000, 17,700 and 18,900 cm^{-1}).[6] This is why distortion of their symmetry, for instance from T_d to C_{3v}, during the formation of the oxygenated $[CoO_3]\cdot O_2$ complex, can manifest itself in a broadening of bands instead of their splitting. This is verified by experiment [Fig. 2(B)]: in comparison with the half-width of bands $\delta_{1/2} = 4800$ cm^{-1} for transitions from the ground ${}^4A_2$ level to ${}^4T_1({}^4P)$ and ${}^2E,{}^2T_1,{}^2A_1,{}^2T_2({}^2G)$ in the 16,000–18,900 cm^{-1} region for the $[CoO_4]$ chromophore in the $NaPO_3$ melt, the half-widths of these bands in the spectrum of oxygenated melts containing cobalt complexes amount to 5000 cm^{-1} [Fig. 2(B)]. This can be due to the splitting of four degenerate levels: ${}^4T_1$, ${}^2E$, ${}^2T_1$ and ${}^2T_2$ (in T_d) into eight levels of *A*- and *E*-types (in C_{3v}) which can be fixed with a common bending line in EAS at high temperature (650°C). An essentially increased intensity of these bands also fits the scheme of the formation of the distorted quasi-tetrahedral mixed-ligand oxygenated complex of cobalt(II).

To ascertain the nature of this complex, let us consider a possible scheme of interaction between the cobalt complex and molecular oxygen in the $NaPO_3$–CoO–O_2 melt in terms of the MO theory.[6]

For the tetrahedrally coordinated $[CoO_3O'_2]$ centre in the metaphosphate melt of oxygenated Co^{II} complexes[6] with the d^7-electron configuration, both the donor transfer of electron density from the $1\pi_u-,3\sigma_g$ MO of molecular oxygen to the orbital of the central ion of cobalt(II) and, especially the acceptor transfer of electron density from the t_2 level of cobalt(II) ion to the half-occupied anti-

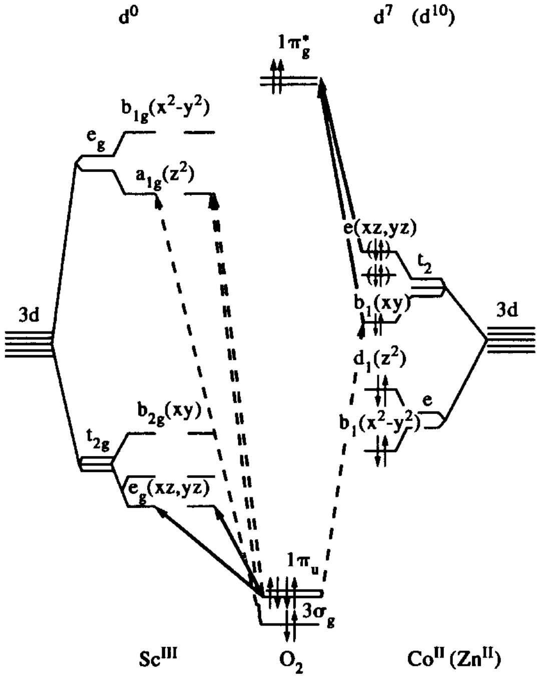

Fig. 3. A simplified scheme of interaction between MO O_2 and *d*-orbitals of the central complexing ion (not to scale).

bonding $1\pi_g^*$-MO O_2, are theoretically possible. In the former case (the complete electron transfer), the formation of the $O_2^{\dot{+}}$ species should be expected, whereas in the latter case, the $O_2^{\dot{-}}$ species is to be formed, both the species possessing an unpaired electron.

To determine the direction of the electron-density transfer the systems of quenched $NaPO_3$–Sc_2O_3–O_2 and $NaPO_3$–ZnO–O_2 melts have been studied by the ESR method.

For the $NaPO_3$–Sc_2O_3–O_2 melt, the Sc^{III} ion (with the d^0-electron configuration) coordinated with oxygen-containing $(PO_3^-)_x$ ligands makes the dative transfer to the $1\pi_g^*$-MO O_2 with the formation of the $O_2^{\dot{-}}$ ion impossible, and an ESR signal could be observed only if the $O_2^{\dot{+}}$ ion-radical is formed. However, for the $NaPO_3$–Sc_2O_3 system, as well as for the $NaPO_3$–$Sc_2O_3+CH_4+O_2$ system, even prolonged bubbling (3600 s) of gases through the melt does not result in the appearance of an ESR signal (Table 1). On the contrary, for the system with the d^{10}-electronic configuration (molten $NaPO_3$–ZnO–O_2), only dative transfer from the filled *d*-orbitals of the Zn^{II} ion to the antibonding $1\pi_g^*$ MO of oxygen is possible with the formation of the $O_2^{\dot{-}}$ superoxide ion (Fig. 3). In passing methane and then air through the $NaPO_3$–ZnO melt an ESR signal ($g = 1.924$, width 42 G) has been observed (Table 1). This fact corroborates our assumption that electron-density transfer from the t_2-level of the cobalt(II) ion to the $1\pi_g^*$-orbital of oxygen proceeds essentially in interaction between molten sodium metaphosphate containing cobalt(II)– and zinc (II)–M complex ions and molecular oxygen. As a result the $[(PO_3^-)_yM\cdot O_2^{\delta-}]$-type oxygenated complex is formed. ESR signals with $g = 1.921$, $g = 1.924$ and widths of 50 G and 42 G in the $NaPO_3$–$Co(PO_3)_x$–O_2 and $NaPO_3$–$Zn(PO_3)_y$–O_2 melts, respectively, different from that for $(PO_3^-)_xO_2$ in the $NaPO_3$ melt ($g = 2.000$), show the somewhat delocalized character of electron-density distribution between the cobalt and zinc ions and the superoxide ion.

Thus, in passing the air or air–methane mixture through both the melt of the individual $NaPO_3$ and the $NaPO_3$–CoO and $NaPO_3$–ZnO systems of melt, superoxide ions of different types ($O_2^{\dot{-}}$ and $O_2^{\delta\dot{-}}$) are formed. In the case of molten systems, coordination of $O_2^{\delta\dot{-}}$ with the central complexing ion in the oxygenated complex is observed, the coordination accompanied by delocalization of electron density between the complexing metal ion and $O_2^{\delta\dot{-}}$. As a result, the value of the *g*-factor decreases.

REFERENCES

1. S. V. Volkov, N. I. Buryak, V. A. Bandur, O. B. Babushkina and A. F. Gurko, *Abstracts of the XIV Mendeleyevskii Congress on General and Applied Chemistry*, p. 293. Tashkent, Uzbekistan (1989).
2. V. A. Bandur, N. I. Buryak and S. V. Volkov, *Abstracts of the V All-Union Meeting on the Chemistry of Non-Aqueous Solutions, Inorganic and Coordination Compounds*, p. 417. Rostov-na-Donu, Russia (1985).
3. S. V. Volkov, V. A. Bandur and N. I. Buryak, *Molten Salt Chemistry* (Edited by M. Chemla and D. Devilliers), p. 273. Trans Tech, Paris (1991).
4. S. V. Volkov, V. A. Bandur and N. I. Buryak, *Teor. Eksp. Khim.* 1991, **27**, 99.
5. S. V. Volkov, V. A. Bandur and N. I. Buryak, *Ukr. Khim. Zhurn.* 1992, **58**, 119.
6. N. I. Buryak, V. A. Bandur and S. V. Volkov, *Zhurn. Neorg. Khim.* 1987, **32**, 2634.
7. R. Jones, D. Summerville and F. Basolo, *Chem. Rev.* 1979, **79**, 139.
8. R. Simoneau, J. Harvey and G. Graham, *J. Chem. Phys.* 1971, **54**, 4819.
9. Yu. Bratushko, *Coordination Compounds of 3-d Transition Metals with Molecular Oxygen*. Naukova Dumka, Kiev (1987).
10. Z. Todres, *Ion-radicals in Organic Synthesis*. Khimiya, Moscow (1986).